

See discussions, stats, and author profiles for this publication at: <https://www.researchgate.net/publication/227927642>

Poly(aryl-ether-ether-ketone) and its advanced composites: A review

ARTICLE *in* POLYMER COMPOSITES · APRIL 1987

Impact Factor: 1.63 · DOI: 10.1002/pc.750080202

CITATIONS

90

READS

65

2 AUTHORS, INCLUDING:



Hatsuo Ishida

Case Western Reserve University

445 PUBLICATIONS 12,673 CITATIONS

[SEE PROFILE](#)

Poly(Aryl-Ether-Ether-Ketone) and Its Advanced Composites: A Review

HUY X. NGUYEN and HATSUO ISHIDA

Department of Macromolecular Science
Case Western Reserve University
Cleveland, Ohio 44106

Poly(aryl-ether-ether-ketone) or PEEK is a highly aromatic semi-crystalline thermoplastic. Its good mechanical properties and solvent resistances rank it as one of the most promising matrix polymers for high performance composites. This article attempts to provide an in-depth review of work on PEEK and fiber-reinforced PEEK composites. Discussions on various areas including synthesis, molecular weight determination, solution properties, structural hierarchy, morphology and mechanical properties of both neat polymer and composites, will be provided. In addition, environmental effects such as physical aging, thermal aging, moisture, solvents, and radiation will be summarized.

INTRODUCTION

Significant progress has been made over the last several years in the development of advanced composites, especially for structural applications in aircraft. The majority of the work has been focused on thermosets such as epoxies or addition type polyimides as matrix materials. However, because of requirements for better mechanical properties and solvent resistance, various thermoplastics are being actively evaluated.

One of them, poly(aryl-ether-ether-ketone) (PEEK), a highly aromatic semi-crystalline thermoplastic, is currently receiving considerable attention. Though high melting, PEEK can be processed on conventional extrusion and injection molding machines. Because of its balanced properties, PEEK may find increasing use in applications such as electrical and electronic parts, military equipment, wires and cables in nuclear plants, underground railways, and oil wells, as well as advanced structural composites for aircraft (1-3).

This paper summarizes recent results in the areas of PEEK and PEEK-based composites. Discussions on various synthesis routes, molecular weight determinations and solution properties, morphologies and mechanical properties of both neat polymer and composites will be provided.

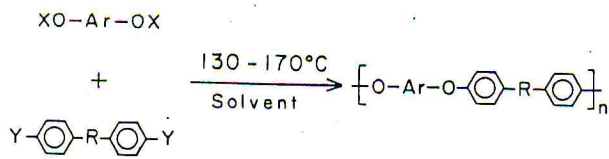
Synthesis

As early as 1967, condensation polymerizations of alkali bisphenates with activated (neg-

atively substituted) aromatic dihalides has been reported by Johnson, *et al* (4). The reaction involves the formation of ether bonds via the nucleophilic substitution of the aromatic dihalides. The work was done as part of a general study on the synthesis of polysulfones and polyethers. The generalized reaction scheme is shown in Fig. 1. This reaction was fast and relatively free of side reactions.

Generally, the cations used were sodium or potassium whereas the halide of choice was fluoride. Only dipolar aprotic solvents at elevated temperatures were found to be useful media for the polymerization reactions. When activated difluorides were used, the reactions proceeded readily in dimethyl sulfoxide (DMSO) at about 160°C. Other sulfone solvents such as dimethyl sulfone and tetramethylene sulfone (Sulfolane) were used when higher reaction temperatures were needed.

Reaction stoichiometry and the exclusion of moisture and air were found to be critical in obtaining high molecular weight polymers. Infrared (IR) and nuclear magnetic resonance (NMR) spectra of the resultant polyethers suggested that only para linkages were formed indicating that the formation of the polymer chains occurred exclusively by a bimolecular process. Most of the resultant polyethers were amorphous thermoplastics with relatively high glass transitions. They were not affected by either aqueous inorganic acids or bases but partially soluble in polar organic solvents such as



Where

X : K or Na

Ar : aromatic group

Y : F or Cl

R : S=O, C=O, N=N, O=S=O

Solvent : DMSO or Sulfolane

Fig. 1. PEEK made by the condensation polymerization of alkali bisphenates and activated aromatic dihalide.

dimethyl formamide (DMF) or N-Methylpyrrolidone.

In this reaction scheme of Johnson, *et al.*, PEEK was made by the reaction of the potassium salt of hydroquinone with 4,4'-difluorobenzophenone in hot Sulfolane. The polymer was crystallizable, with the glass transition (T_g) around 160°C and the melting transition (T_m) around 350°C.

Because of its crystallinity, which makes it very insoluble in most solvents, the growing poly(aryl-ether-ether-ketone) chains precipitate from solution and growth stops, resulting in low molecular weight polymers (5). It was not until diphenyl sulfone was used as solvent for the polycondensation reaction of 4,4'-difluorobenzophenone and the potassium derivatives of hydroquinone by Attwood, *et al.* (6) that high molecular weight PEEK was made. However, temperatures as high as 335°C were needed for such reactions (Fig. 2). The T_g and T_m of the resultant polymer were determined by differential scanning calorimetry (DSC) to be around 145 and 335°C, respectively. The lower T_g and T_m of this supposedly higher molecular weight polymer [compared to the one made by Johnson, *et al.* (4)] could be due to its molecular weight distribution.

Recently, Kricheldorf and Bier (7) carried out bulk condensations of various silylated bisphenols and 4,4'-difluorobenzophenone at elevated temperatures (220 to 350°C), using cesium fluoride as the catalyst. Nucleophilic aromatic substitution was also the mechanism. Transesterifications were not found during the course of the polymerization.

The most effective amount of cesium fluoride catalyst was found to be of the order of 0.1 percent by weight with respect to the total weight of the monomers. Thus all anions which form insoluble cesium salts (such as chloride ions) must not be present during the reaction. This could be a disadvantage since the silylation of the bisphenols required the use of chlorotrimethylsilane and triethylamine in boiling toluene. Extreme care must be taken because amine hydrochlorides, a product of the silyla-

tion reaction, could contaminate the silylated bisphenols.

A major advantage of the reaction procedure of Kricheldorf and Bier was that purification of the molten polymer from solvents or metal salts was not required. The reaction scheme to make a semi-crystalline PEEK, which is soluble in concentrated sulfuric acid, is shown in Fig. 3.

As can be seen in Figs. 1 to 3, the molecular structure of PEEK is rather simple. There are only two types of linkages in the chains, ether and ketone. Most of the research on the physical and mechanical properties of PEEK, as well as its composites, were done using various commercial grades of PEEK (VICTREX by ICI). The grades used for films, wire covering, and injection molding seem to require very slow cooling or post annealing to obtain the optimum crystalline content. The grades used in APC (Aromatic Polymer Composites, composites of PEEK and carbon fibers made by ICI) were claimed to give consistent crystalline content (~35 percent) when cooled rapidly from the melt to the temperature range of 20 to 200°C (29).

SOLUTION PROPERTIES AND MOLECULAR WEIGHT DETERMINATIONS

Until recently, all the research on solution properties of PEEK has been limited to solution viscosity measurements due to the insolubility of the polymer in common solvents. In a typical study, as represented by the one by Attwood, *et al.* (6), attempts were made to correlate the reduced viscosity (RV) and inherent viscosity (IV) with the fracture toughness of a compression molded PEEK film. The viscosities are defined in Table 1. Reduced viscosities were measured in Ostwald viscometers at 25°C using a solution of 1.00g polymer per 100ml 98 percent sulfuric acid. Inherent viscosities were calculated from the values of specific viscosity at 0.1g/ml. They found that tough, partially crystalline film can

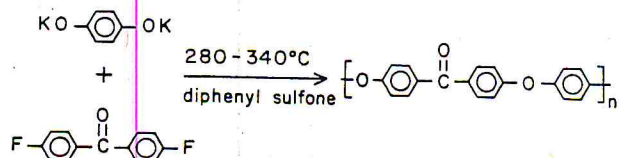


Fig. 2. PEEK made by the reaction of 4,4'-difluorobenzophenone and the potassium derivatives of hydroquinone.

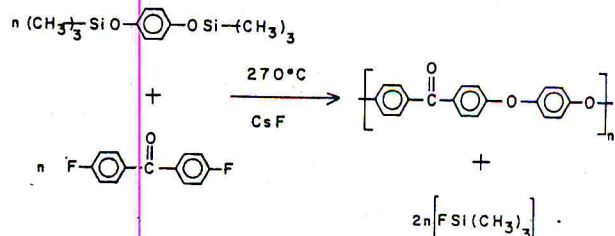


Fig. 3. PEEK made from silylated bisphenols and 4,4'-difluorobenzophenone.

Table 1. Definitions of Viscosities.

Symbol	Definition
η_o	Viscosity of a pure solvent
η_s	Viscosity of a dilute solution with concentration c
$\eta_r = \frac{\eta_s}{\eta_o}$	Relative viscosity
$\eta_{sp} = \eta_r - 1$	Specific viscosity
$(RV) = \frac{\eta_{sp}}{c}$	Reduced viscosity
$(IV) = \frac{\ln \eta_r}{c}$	Inherent viscosity
$[\eta] = \lim_{c \rightarrow 0} (RV)$ $= \lim_{c \rightarrow 0} (IV)$	Intrinsic viscosity

be compression-molded when the polymer's RV is greater or equal to 1.03 (which corresponds to $IV > 0.8$), indicating that the molecular weight of their polymer was in the useful range. The commercialized polymer has RV in the range of 2.3.

In addition to strong acids (H_2SO_4 , HSO_3Cl , CH_3SO_3H , and HF), other researchers have recently found that at elevated temperature, PEEK can be dissolved in high-boiling esters (8), diphenyl sulphone (8), benzophenone (8, 9, 10, 12), α -chloronaphthalene (10), and a mixture of phenol and 1,2,4-trichlorobenzene (TCB) (11, 12) at concentration ranges from 0.001 to 0.1 percent. Del Rios (11) showed that the molecular weight of PEEK can be measured by gel permeation chromatography (GPC) at elevated temperatures. Using a Waters 150C GPC with Ultrastyragel columns operated at 145°C, he claimed to obtain results with good reproducibility for a 1g/L solution of PEEK in a 1:1 solvent mixture of TCB and phenol.

Detailed studies of properties of PEEK in dilute solutions have also been reported (12, 13). In concentrated sulfuric acid and chlorosulfonic acid, PEEK became sulfonated to an equilibrium level of one $-SO_3H$ per structural repeat unit in less than one day. Sulfonation strongly influences the solution properties of PEEK by, in effect, increasing its molecular weight, and must be taken into consideration. Devaux, *et al* (12) characterized a number of PEEK samples by light scattering, viscometry, and GPC. They showed that both melt and intrinsic viscosities of PEEK vary as power functions of molecular weights (apparent M_w). The adequacy of power functions as one of the model to describe the relationship between intrinsic viscosity and apparent M_w by light scattering was also pointed out by Bishop, *et al* (13). Light scattering and intrinsic viscosity data of PEEK in concentrated sulfuric acid from both studies are reproduced in Table 2 for comparison purposes. Whether the slightly different experimental procedures can account for the large discrepancy between the two sets of data is not certain.

Table 2. Weight-Average Molecular Weight, Radius of Gyration, and Intrinsic Viscosity of PEEK in Concentrated H_2SO_4 .

Apparent weight-average molecular weight by LS (M_w) ^a	Apparent radius of gyration by LS (A°) (R_g) ^a	Intrinsic viscosity $[\eta]$ (dL/g)
14,300 ^a	155 ^a	0.45 ^a
22,600 ^a	190 ^a	0.80 ^a
28,300 ^a	200 ^a	0.92 ^a
31,800 ^b	155 ± 40 ^b	0.716 ± 0.002 ^b
37,200 ^a	220 ^a	1.37 ^a
52,000 ^b	204 ± 26 ^b	0.931 ± 0.003 ^b
56,500 ^a	280 ^a	1.59 ^a
57,100 ^b	212 ± 22 ^b	1.124 ± 0.005 ^b

^a Data by Devaux, *et al.*; a He-Ne laser at 632 nm was used in light-scattering experiments.

^b Data by Bishop, *et al.*; an Ar laser at 514.5 nm was used in light-scattering experiments.

The description which emerged from the work of Bishop, *et al* (13) for dilute solutions of PEEK in concentrated H_2SO_4 is that the PEEK molecule can best be represented as a "partially draining wormlike coil, perhaps with excluded volume." Increased aggregation or expansion of the coils in stronger acids, with the potential occurrence of crosslinking reactions, was also indicated.

Solution viscosity and GPC measurements of PEEK in a Phenol/TCB solvent mixture at 115°C were also reported by Devaux, *et al* (12). They calculated the weight average molecular weights of the PEEK samples based on a universal calibration curve. This curve was constructed from the Mark-Houwink equation for polystyrene standards and the GPC molecular weights of these samples. They found the agreement between the M_w by GPC (solvent; Phenol/TCB) and the apparent M_w by light scattering (solvent; concentrated sulfuric acid) is fairly good (<8 percent) for the low molecular weight samples but the differences are up to 20 percent for the highest one.

MORPHOLOGY OF NEAT POLYMER

Numerous studies of the melting, crystallization and crystallization kinetics, and the morphology of PEEK have been reported. Techniques such as X-ray, IR spectroscopy, Raman spectroscopy, DSC, dynamic mechanical analysis (DMA), optical microscopy, and electron microscopy have all been used to some extent.

Melting Behavior

The melting behavior of PEEK has been studied by DSC (14, 16) and by Fourier transform infrared (FT-IR) spectroscopy (15, 16). Typical DSC traces of PEEK are shown in Fig. 4 (17). Upon heating at 10°C/min, a glass transition (T_g) at around 145°C, an exothermic peak, $T_{c,h}$, (associated with crystallization) at about 180°C, and a melting endotherm, T_m , at about 335°C, were found. The cooling scan of Fig. 4, also at 10°C/min, shows a crystalline exotherm ($T_{c,c}$) at

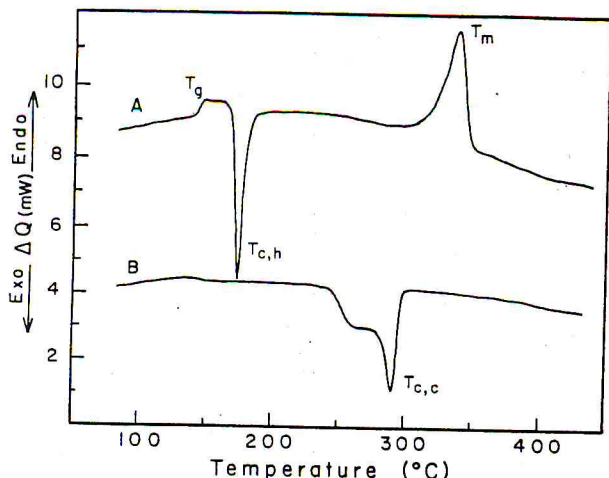


Fig. 4. Typical DSC thermograms of PEEK: (A) amorphous polymer upon heating at 10°C/min; (B) cooling scan at 10°C/min. Data from (17).

about 290°C with a broad shoulder at about 260°C. This indicates that crystallization of PEEK may follow a 2-stage process, depending upon the cooling rate.

The intensity and the shape of the crystalline exotherm depend strongly on previous processing history (melt temperature, crystalline content, etc.) (16, 18). In fact, it has been shown that depending upon previous crystalline temperatures, two melting processes can take place (14, 19). The smaller, lower-temperature endotherm is associated with the continuous melting and recrystallization of the crystallites which were previously formed at lower temperatures. Its position varies anywhere from 10°C above $T_{c,h}$ to a shoulder of T_m . On the other hand, T_m varies only slightly with prior crystalline content and, thus, is more characteristic of PEEK itself.

Local order in the disordered phase of PEEK was observed in the melt, up to a melt temperature of 400°C (45°C above $T_m = 335^\circ\text{C}$). This local order was found to be associated with the diphenyl ether segments of the PEEK chains (15, 16). These relatively ordered regions in a polymer melt may act as nucleating sites, which further complicates its crystallization behavior. In fact, changes in the nucleation density as a function of the temperature at which the melt was heated (between 380 and 400°C or above) has been observed (23, 25). However, PEEK was found to be neither a thermotropic nor a lyotropic (in benzophenone) liquid crystal (20). The next transition of PEEK observable by thermal analysis is the decomposition temperature. Its onset has been detected by thermogravimetry to be around 560°C (21).

Assessment of Crystallinity

Major effort has been placed on the calculation of crystalline content and the elucidation of crystallization kinetics of PEEK, for the obvious reason that the percent crystallinity

strongly influences the mechanical properties of the polymer. Most of the crystallinity measurements were done via wide-angle X-ray diffraction (WAXD) (14, 22–24) and DSC (16, 18, 19, 25). But work with FT-IR (16, 24, 26), Raman (27), and NMR (28) spectroscopies have also been reported.

Blundell and Osborn (14) compared the estimated crystalline content of PEEK from WAXD and its specific volume as measured on a density column. The extrapolated densities of 100 percent amorphous and 100 percent crystalline (density of the observed unit cell) samples were calculated to be 1.260 and 1.400 g/cm³, respectively. Depending on the processing conditions, crystalline content has been found to vary from 0 to 40 percent by X-ray, DSC, and density measurements. Table 3 shows the dependency of absolute crystalline content on processing conditions. Typical crystalline content of PEEK in a 50 percent carbon fiber composite is 35 percent as determined by DSC (29).

In a preliminary study, Clark, et al (28) pointed out that by using different pulse sequences in a NMR experiment, band assignments of specific carbons of the PEEK chains in the solid state can be elucidated. They indicated that a study of the degree of crystallinity of PEEK on both sides of its T_g is possible once the characterization of the different carbons in the solid state is completed.

Using multiple internal reflection infrared (MIR-IR) spectroscopy, Chalmers, et al (26) attempted to correlate the intensity ratios of a number of absorption bands with the crystal-

Table 3. The Influence of Processing Conditions on the Crystalline Content of PEEK.

Processing Conditions	Crystalline content (%)		
	Density Measurement	X-ray	DSC
As received polymer			33 ^c
Quenched from 400°C	0 ^a	0 ^{a,b,d}	17 ^{c,d}
Quenched from 380°C			23 ^c
Quenched from 370°C			23–25 ^e
Quenched from 400°C, then annealed at 200°C			21 ^b
Crystallized at 155°C, then annealed at 200°C	27 ^a	25 ^a	
Quenched from 400°C, then annealed at 230°C			26 ^b
Quenched from 400°C, then annealed at 270°C			29 ^b
Crystallized at 310°C			32 ^b
Crystallized at 320°C			40 ^b
Crystallized at 325°C	35 ^a	30 ^a	
Cooled from 420°C to room temperature			38 ^f
Cooled from 400°C to room temperature			43 ^f
Cooled from 380°C to room temperature			22 ^f
			23 ^c

^a Hay, et al., Ref. 22.

^b Blundell and Osborn, Ref. 14.

^c Nguyen and Ishida, Ref. 16 (crystalline content developed upon heating).

^d Kemish and Hay, Ref. 18.

^e Cebe, Ref. 19 (crystalline content varies with heating rate).

^f Kumar, et al., Ref. 23.

line contents which were measured by WAXD. Typical MIR-IR spectra of PEEK samples which has various degrees of crystallinity are shown in Fig. 5. Plots of the intensity ratio of the bands at 1305cm^{-1} and 1280cm^{-1} and that of the bands at 970cm^{-1} and 952cm^{-1} , vs. the crystalline contents of molded plaques show linear relationships. In a later study of APC-2 composites (Hercules AS4 carbon fiber reinforced PEEK) (24), they decided that the intensity ratio of the bands at 966cm^{-1} and 952cm^{-1} is preferred as the indicator of the crystalline content. Similarly, Louden (27) studied the crystallinity of PEEK films using the intensity ratios of various bands of their Raman spectra (Fig. 6). He found linear correlations between the crystalline contents by MIR-IR and the relative intensity ratios of $830\text{cm}^{-1}/810\text{cm}^{-1}$, and $1600\text{cm}^{-1}/1610\text{cm}^{-1}$. A potential source of error of this technique is the extremely low intensities of the IR bands chosen for the ratioing step.

A different approach was taken by Nguyen and Ishida (16). From the FT-IR spectra of cast films with widely different crystalline contents, "spectroscopically pure" spectra of the crystalline and amorphous phases of PEEK were cal-

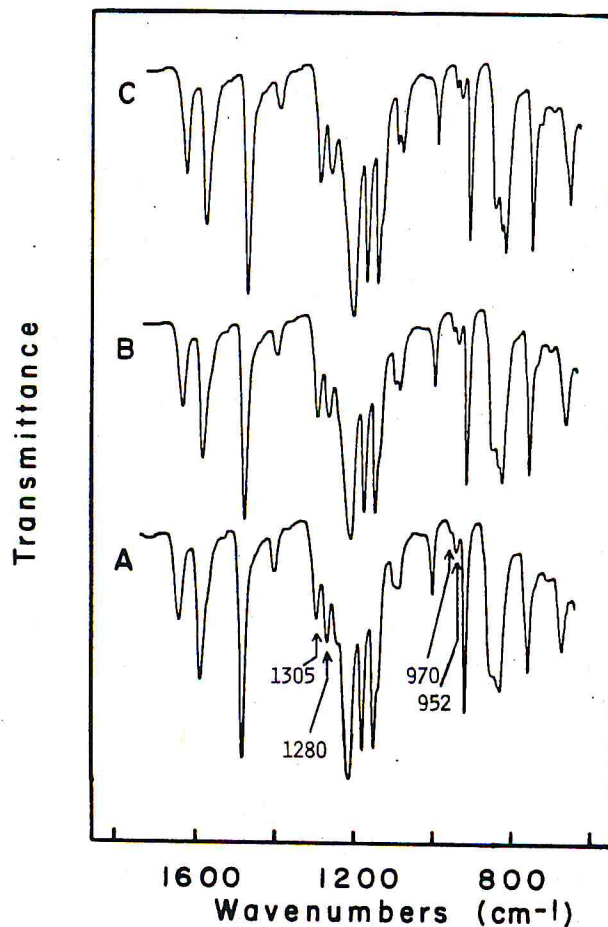


Fig. 5. Multiple internal reflection infrared (MIR-IR) spectra of compression molded plaques: (A) amorphous; (B) 26 percent crystalline; (C) 40 percent crystalline. Reproduced from data of Chalmers, et al. (26).

culated (Fig. 7). Then applying a least square curve-fitting algorithm to the digitized spectral data, assuming that there are only two phases (amorphous and crystalline) present in a semi-crystalline PEEK sample, its crystalline content could be calculated. The results from this technique were generally higher than those obtained via X-ray or DSC techniques, which indicates that the contributions of "crystalline-like" conformers in the disordered phase were also detected. Tentative IR band assignments of PEEK and its model compounds have also been reported (17).

Crystallization Kinetics

The overall crystallization rate of PEEK quenched from 400°C , as measured by DSC, goes through a maximum at around 230°C (14). When the polymer was annealed, the crystal

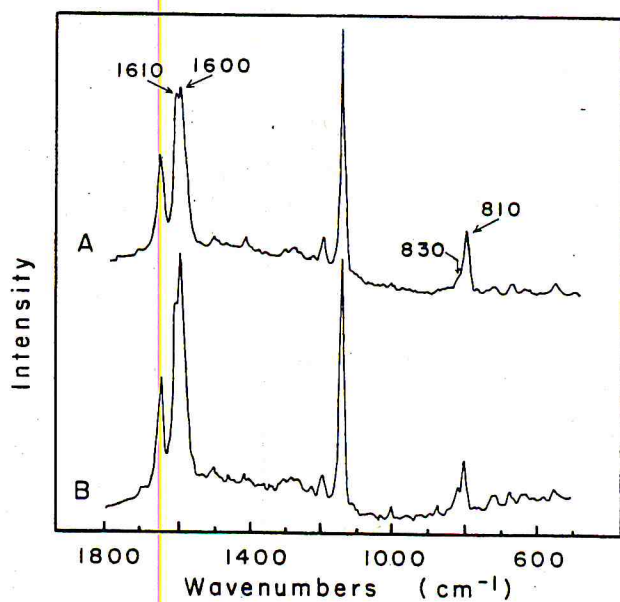


Fig. 6. Raman spectra of PEEK films: (A) Amorphous; (B) semi-crystalline. Reproduced from (27).

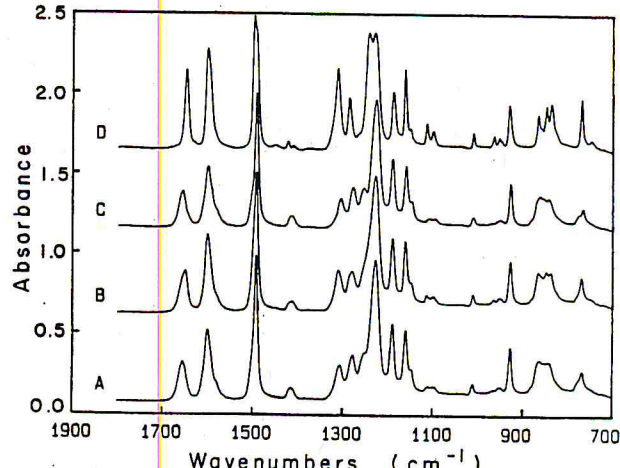


Fig. 7. FT-IR transmission spectra of PEEK films: (A) quenched sample; (B) annealed sample; (C) amorphous phase; (D) crystalline phase. Data from (16).

growth rates were reported to fit Regime I kinetics. The linear growth rates were found to be 161, 264, 540, and 980 nm/s when the annealing temperatures were 287, 277, 260, and 240°C, respectively (14). Using optical microscopy, Kumar, *et al* (23) studied isothermal crystallization at 300 and 320°C for polymer melt at 380 and 420°C. Nucleation density was so high, if the melt temperature was 380°C, the crystallization could not be monitored visually. For polymer melt at 420°C, the linear crystal growth rates were found to be 320 and 45 nm/s at annealing temperatures of 300 and 320°C, respectively. These growth rates are higher compared to those reported by Blundell and Osborn (14).

Various forms of the Avrami equation have been used to model crystallization kinetics of PEEK (18, 19, 30). Below T_g , two molecular movements preceding isothermal crystallization via annealing were observed by FT-IR (30). In the temperature range of 50 to 140°C, the partial rotation of the ether linkages to allow better chain packing was reported. The second conformational change, which requires the motion of the whole chains (crystallization) and occurs around T_g , can be modeled by an Avrami equation with an Avrami constant $n = 1.0$. This indicates that at around T_g , predetermined fibrillar crystal growth or secondary crystallization may be the controlling mechanism. Immediately above T_g , PEEK was observed by DSC to crystallize isothermally at increasing rates as the annealing temperature increased. The Avrami constant n was found to be approximately 3.0, which is consistent with spherulites heterogeneously nucleated (18). However, the crystal growth rate was found to be diffusion-controlled rather than nucleation-controlled (18). Non-isothermal crystallization from 80 to 380°C, with rates from 1 to 50°C/min was investigated by Cebe (19), using DSC. The Avrami constant n was found to vary from 4.7 to 7.8, indicating a stronger time dependence of crystal growth rate. Cebe (19) reported an activation energy of the primary crystallization process of 0.22 MJ/mole, whereas Kemmish and Hay (18) found it to be 1.35 MJ/mole.

Spherulitic Structure

It is generally accepted that PEEK forms spherulites in the bulk when it is crystallized from the melt. The morphology within the spherulites depends strongly on the temperature at which crystallization occurs during the fabrication process. The range of temperature for optimum crystallization has been reported to be 180 to 320°C (31). Spherulitic radii ranges from 12.7 to 21.9 μm for crystallization temperatures of 240 and 287°C, respectively, have been obtained (14). The cooling rate from the melt to room temperature is also important. For cooling rates faster than 2000°C/min, so little

crystallization can take place that the polymer will essentially be amorphous. For cooling rates faster than 700°C/min, the spherulitic growth is retarded. Small spherulites are formed with amorphous polymer remaining between the spherulites. Post-annealing at 200 to 300°C for about 30 min will produce a satisfactory degree of crystallinity (31). However, the spherulite size is expected to remain unchanged.

Both positive birefringence (14) and negative birefringence (23, 32) have been observed to associate with the spherulites. Whether there are two different types of spherulites depending upon the annealing conditions remains to be addressed.

The Bragg long period as deduced from small-angle X-ray scattering (SAXS) increases with increasing crystallization temperature. At a low crystallization temperature of 200°C, the crystal thickness (calculated from the long period) was found to be only around 2.0 nm. A crystal thickness of 5.9 nm has been achieved by annealing PEEK at 320°C for 16 h (14). Since the length of a repeat unit is around 1.5 nm, at lower crystallization temperature, the chains must pack with the ketone and ether linkages arranged randomly with respect to each other.

Other types of crystals have also been observed. When PEEK was crystallized isothermally from solution (solvent was either benzophenone or α-chloronaphthalene), single crystals, axialities, and spherulites were obtained (10). The single crystals are elongated and spear-like, which actually consist of much narrower microcrystals. In general, the length of the single crystals is 1 to 3 μm, and their width is about 0.1 to 0.3 μm. Electron diffraction patterns indicated that the molecular chains are oriented in the thickness direction of the single crystals.

Thin films of PEEK crystallized from the melt may lead to the growth of full spherulites having essentially cylindrical symmetry (Fig. 8) (32). Row nucleation was also observed when a sample was fast cooled (but not quenched) from the melt at 400°C to room temperature (23).

Oley, *et al* (33) had developed an etching technique for studying the lamellar and spherulitic morphology of PEEK under electron microscope. They found that for samples crystallized isothermally, after cooling from the melt down to the crystallization temperature, spherulites with stacks of lamellae were seen. The periodicity of the lamellae were found to be about 15 nm. In addition, sheaf-like spherulitic precursors were also seen. On the other hand, samples crystallized via annealing from the amorphous state produced spherulites an order of magnitude smaller. Lamellae were found to be thinner and smaller than those obtained from melt-crystallization. Higher nucleation density was probably the reason for this reduction in lamellar size.

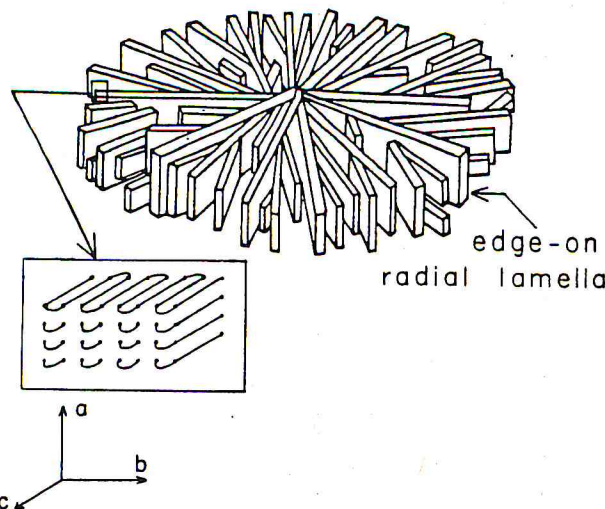


Fig. 8. Schematic representation of a spherulite with cylindrical symmetry in a PEEK thin film (few hundred nanometers thick film).

Unit Cell

X-ray diffraction data of unoriented film (23, 26), plaque (22, 34), oriented then annealed sheet (22), fiber (34), and die-drawn rod (35) samples of PEEK have shown that the unit cell is orthorhombic. The reported values of a, b, c axes (with c is the fiber axis) of the cell range from $a = 0.775$ to 0.788nm , $b = 0.586$ to 0.594nm , and $c = 0.988$ to 1.007nm . The unit cell is generally considered to contain only two thirds of a repeat unit (Fig. 9). However, a unit cell with $c = 3.050\text{nm}$, which contains 2 repeat units, has also been proposed (31). The planes of all the molecular zig-zag backbones were found by electron diffraction to be parallel to the b-axis (10). The reported values of the calculated crystal density also varies from 1.341g/cm^3 to 1.415g/cm^3 . Orientation induced by drawing processes were found not to alter the unit cell parameters (35).

A schematic representation of a spherulite is shown in Fig. 10. Diffraction patterns revealed that the b axis is radial, while the a and c axes are tangential, with respect to the PEEK spherulite (23). Since the growth direction is radial, the preferred growth direction (the direction of the worm-motion within a fold plane) in PEEK spherulites should be along the b axis. Indeed, this was found to be the case in solution-grown single crystals (10) and melt-crystallized spherulites (32). The a-axis is then perpendicular to the fold plane, which in this case is also the molecular zig-zag plane. However, Kumar, *et al.* (23) observed that the growth faces of the crystallites and the radial direction of melt-crystallized spherulites are about 55° instead of perpendicular. They suggested that the (110) is the preferred crystal growth plane.

In the crystalline domains (i.e. crystal unit cells), the PEEK chains adopt an extended conformation. The phenyl rings form alternating

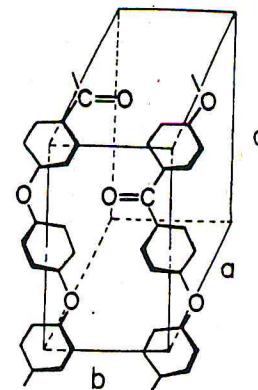


Fig. 9. Schematic representation of an orthorhombic unit cell which contains two thirds of a repeat unit of PEEK.

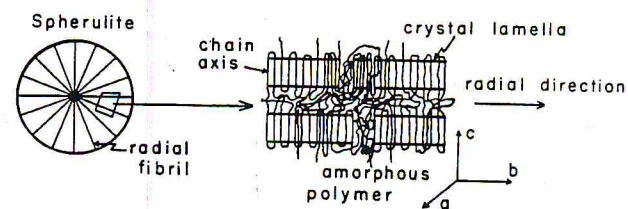


Fig. 10. Schematic representation of an undeformed spherulite.

angles of about $\pm 40^\circ$ with respect to the plane of the zig-zag backbone (32). From the view point of chain packing, the ketone and ether linkages can be interchanged with only minimum distortion.

MORPHOLOGY OF PEEK IN COMPOSITES

The presence of foreign surfaces strongly influence the morphology of PEEK. The nucleation of a polymer on substrates can be complex, depending upon factors such as surface energies of the substrates, temperature gradient, unit cell dimensions, shear field, etc. The interactions of PEEK and graphitic substrates are of particular interest since carbon fiber reinforced PEEK composites have significant commercial importance.

PEEK was found to crystallize at higher temperatures (lower supercooling, smaller ΔT) with higher nucleation densities as the fiber content of a carbon fiber reinforced composite was increased (25). This suggested that the fiber surfaces act as nucleating sites. The spherulites grow around the fibers and terminate when impingement, either between the spherulites or between the spherulites and the fibers, occurs. The average size of spherulites in APC-1 (a PEEK composite with approximately 50 percent Courtauld XA-S carbon fiber by volume) is about $2\mu\text{m}$ (29). Prior thermal history seems to influence the isothermal crystallization of neat PEEK more than that of carbon fiber reinforced PEEK (25).

The microstructural feature which is a significant factor in determining the properties of

PEEK composites is transcrystallinity, which is the columnar growth of crystals (on the order of 10 to 50 μm) perpendicular to the fiber surfaces. Optical micrographs of fractured sections of APC-1 show the fibers always coated with PEEK, as evidence of the strong interfacial interaction caused by transcrystallinity at the fiber surfaces (29, 39). Transcrystallinity has also been associated with the increase in deflection temperature under load (DTUL) when PEEK was reinforced with glass and carbon fibers (37). The dimension of the transcrystalline regions, not the total content, seems to be the controlling factor. The increase in DTUL could be as high as 152°C (from 160 to 312°C) and 161°C (from 160 to 321°C) for 30 percent loading of glass fiber and carbon fiber, respectively. In highly-loaded composites (50 to 70 percent fiber by volume), adjacent transcrystalline regions may impinge on each other, their boundaries may become areas of weakness and be susceptible to long term failure (38).

In carbon fiber reinforced composites with unsized Thornel 300 (a PAN-based carbon fiber made by Union Carbide), long melt-annealing time (holding time in the melt) was found to favor transcrystallinity (25). Shear flow during processing can also induce transcrystallinity (38). However, the factor most influential to the formation of transcrystallinity is the nature of the substrate. Hartness (39) found that transcrystallinity is the predominant growth only if the carbon fibers have large (~10.0 nm) graphite basal planes that are highly oriented along the fiber axis. On the other hand, spherulites nucleated and grew equally well in bulk if turbostratic graphite structures with small graphite planes (~2.5 nm) and a high degree of dis-orientation were used.

The influence of the substrate on the directional crystallization of PEEK is even more pronounced if the surface is fully crystalline. The interfacial interaction of PEEK and the basal plane (001) of graphite single crystals was investigated by Nguyen and Ishida, using FT-IR (9). PEEK melt quenched on the basal plane of a graphite single crystal did not show preferred orientation. However, when the thin polymer film was annealed above its $T_{c,h}$, the chains were found to crystallize perpendicularly to the substrate. The thicker the film (up to about 38 nm), the higher the temperature or longer annealing time was needed to complete the orientation process. Based on the pictures of the unit cell and lamellar morphology (Figs. 9 and 10), the lamellae induced by the basal plane of a graphite single crystal should be rigid, narrow, and flat (i.e., parallel to the substrate). They may be very similar to the individual crystals (width = ~15 to 20 nm) found in solution-grown PEEK single crystals (10, 40). Their a and b -axes are tangential, with b as the preferred growth direction. The growth plane is perpendicular to the substrate.

Uniplanar growth of PEEK lamellae was also observed on freshly cleaved mica by Lovinger and Davis (32), using electron diffraction. A slightly different type of growth was found. The lamellae were observed to be essentially on edge, with the lamellar height approximately 250 nm. The b -axis was radial and the preferred growth direction; therefore, the growth direction is parallel to the substrate. The c -axis is tangential while the a -axis is perpendicular to the spherulitic plane (a -axis is the height direction of the lamella standing on edge). It should be noted here that transcrystalline growth on a surface yields still a different morphology; the lamellae are on edge, but the growth direction (and the growth plane) is now perpendicular to the substrate. Schematic representations of the three different lamellar orientations are given in Fig. 11.

Lovinger and Davis also found lamellae in a flat-on orientation "... in open regions of the films, particularly within the spherulitic eyes on either side of the nuclei." Whether these flat lamellae are of the same nature as the ones observed to crystallize on the basal plane of graphite single crystals is not clear at the present time.

Blundell, et al. (24) found that upon cooling from the melt at 380°C, the crystalline content of PEEK in APC-2 composites increased slowly with decreasing cooling rate. Only about 25 percent crystallinity was achieved when the cooling rate was around 500°C/min, whereas about 40 percent was obtained if the sample was cooled by 0.5°C/min. When amorphous samples were annealed, the crystalline content increased slightly from about 22 to about 26 percent when the annealing temperature was increased from 200 to 300°. Only when the composite sample was annealed at 320°C would the crystalline content of the matrix exceed 35 percent. Lee and Porter (25) reported quite higher crystalline contents in composites of PEEK reinforced with Thornell 300 fiber. For samples cooled from 390°C to room temperature, they obtained from 36 to 45 percent crystallinity (by DSC) for samples with fiber con-

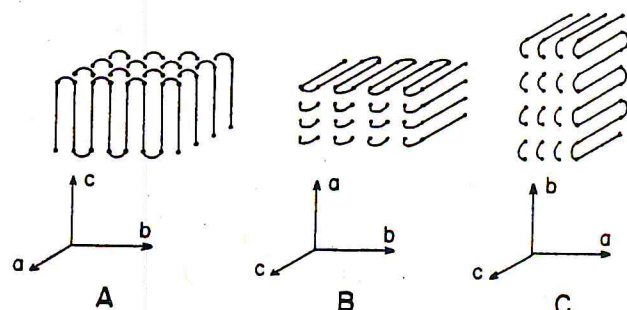


Fig. 11. Proposed orientations of lamellae in films with different thicknesses: (A) thickness on the order of tens of nanometers; (B) thickness on the order of hundreds of nanometers; (C) thickness on the order of tens of micrometers (transcrystalline regions).

tents varying from 11 to 32 percent by volume, respectively.

MECHANICAL PROPERTIES OF NEAT POLYMER AND COMPOSITES

There have been numerous papers on the mechanical properties of PEEK and its fiber-reinforced composites, including short glass fibers, short carbon fibers, continuous carbon fibers, and woven carbon cloths. In general, the addition of reinforcing fibers introduce anisotropy, increase tensile strength and modulus, while drastically reduce tensile elongation.

While fiber-reinforced PEEK exhibits brittle fracture behavior because of the domination of the fiber, the neat polymer exhibits yielding or shear banding (42), indicating its ductility. The plastic zone size was found to be greater than $20\mu\text{m}$ (29). The yield stress follows an inverse linear relationship with temperature. It was found to be about 170 and 70MPa at -80 and 60°C , respectively. Typical reported room temperature tensile properties of unreinforced PEEK are: tensile yield stress = 100MPa, tensile modulus = 4GPa, and tensile elongation = 150 percent. The brittle-to-ductile transition of PEEK was found to be around -15°C .

The fracture toughness of PEEK has been studied via fatigue tests of notched and unnotched samples (41, 42), and three-point bend tests using single-notched specimens (42). Dynamic stress allows flaws to grow and precipitate into cracks. It also minimizes plastic deformation (the off-load periods allow some strain recovery) which, in turn, lowers strength and ductility. Jones, *et al.* (42) found this is the case with PEEK. They also found that notched specimens had a much lower degree of ductility compared to that of the unnotched ones. Figure 12 illustrates typical fatigue behaviors of injection molded neat PEEK specimens.

The advancing fatigue cracks were found to prefer transpherulitic (through the middle of the spherulites) paths, without the presence of fatigue striations (41). Using linear elastic fracture mechanics, Jones, *et al.* (42) obtained the intrinsic toughness parameter (geometry independent): critical stress intensity factor, $K_{IC} = 3.3\text{MN.m}^{-3/2}$, and critical strain energy release rate, $G_{IC} = 4.8\text{kJ.m}^{-2}$.

Creep tests allow the time-dependent behavior of modulus (stiffness) to be studied. Jones, *et al.* (42) carried out creep tests of PEEK for approximately one year in the temperature range of 20 to 180°C . They found that tensile creep modulus depends strongly on temperature but only slightly on time, indicating the excellent creep resistance of PEEK (Fig. 13). They also developed a simple 3-D plot, correlating creep modulus, temperature and time, which may be useful as design guideline for long-term stiffness.

When short fiber reinforced PEEK is injection

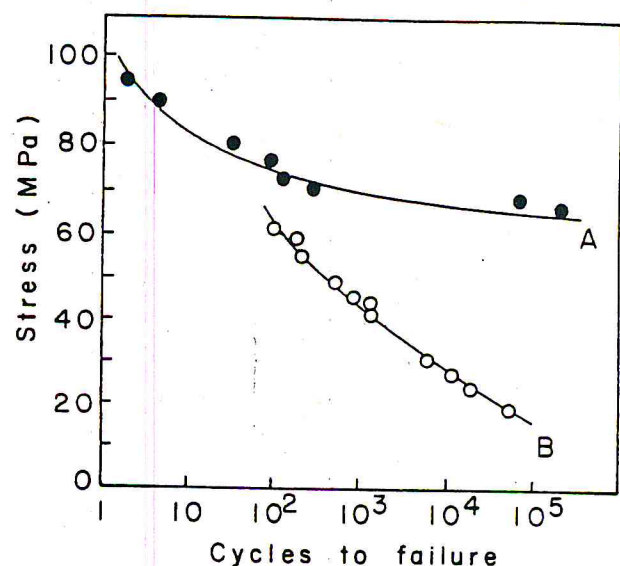


Fig. 12. Fatigue behavior of unreinforced injection molded specimens. Tests were done in transverse direction: (A) unnotched samples; (B) notched samples. From data of Jones, *et al.* (42).

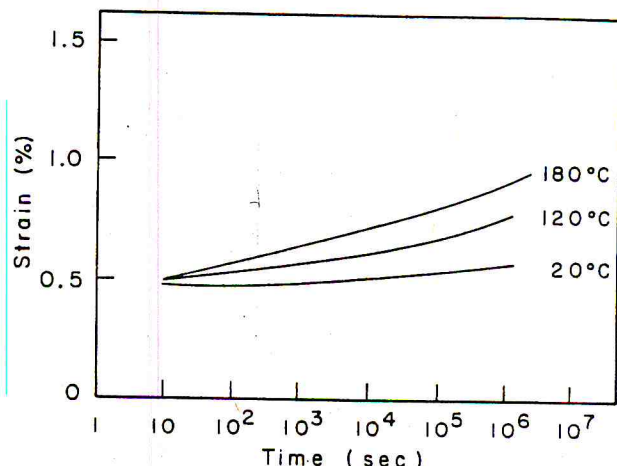


Fig. 13. Tensile creep curves at different temperatures. Applied stresses were 20, 18, and 2.4MPa at 20°, 120°, and 180°C, respectively. Data from (42).

molded, the fibers in the skin are aligned predominantly along the mold fill direction (MFD), while transverse fiber orientation exists only in a relatively thin (about 4 percent of total thickness) central core (42, 43). That allows a certain level of anisotropy to exist in 30 percent short fiber reinforced specimens. For example, Yau and Chou (43) found the tensile strength and modulus of 2mm thick E-glass fiber reinforced plaques to be 128MPa and 29.1GPa in the MFD, and 86.9MPa and 22.1GPa in the transverse direction. The degree of anisotropy in tensile properties (ratio of a tensile property in the MFD to that of the transverse direction) was found to be higher in short carbon composites compared to that of short glass fiber composites (1.7 vs. 1.4 (42)). Flexural properties are dominated by the skin of a molded specimen. Hence, the longitudinal flexural strength should be highest. This was found in the case of short glass fiber

reinforced PEEK by Jones, *et al.* (42). However, they found a surprising result that the flexural strength of short carbon fiber reinforced PEEK is dominated instead by the small amount of fibers aligned transversely in the core of the specimens.

Pao, *et al.* (41) compared the tensile properties and fracture toughness of PEEK specimens reinforced with either 30 percent by weight of a short E-glass fiber or a polyacrylonitrile (PAN) based short carbon fiber. They found that the E-glass fiber marginally improves the tensile strength (from 100 MPa for neat PEEK to 110 MPa) whereas a 50 percent increase in tensile strength was observed with the short carbon fiber reinforcement. The fracture toughnesses of the two composites were found to be comparable with that of the neat polymer (8.6 to 8.9 MPa.m^{1/2}), but the ultimate tensile elongation of each composite dropped by about 75 percent (from 28.5 to about 7.4 percent). Jones, *et al.* (42), however, found the short glass fiber reinforced composite had a larger total fracture energy than that of the short carbon fiber reinforced material. The difference was in the propagation energy, which is higher for the glass fiber reinforced PEEK. They associated this phenomenon with the more anisotropic nature of the carbon fiber reinforced composite.

The fatigue crack growth resistance of the composite was not improved by the addition of E-glass fibers, whether the samples were notched (41) or unnotched (44). Poor bonding at the interface of the glass fiber and PEEK was believed to be the cause. On the other hand, the addition of carbon fibers significantly improved fatigue crack resistance (the fatigue crack growth rate was found to be 4 to 6 times lower than that of neat PEEK, depending on the stress intensity level). This increase was attributed to the good carbon fiber/PEEK interfacial adhesion. The crack growth rate became more stress dependent, however. As in the case with neat PEEK, dynamic stress was found to reduce the toughness of the short fiber reinforced composites (42).

Composites made from continuous carbon fiber reinforced PEEK laminates have, in general, better properties than those of short carbon fiber reinforced composites. Most of the work has been done with either APC-1 or APC-2 (products of ICI). However, prepgs made with other types of carbon fibers have also been tested. Usually, the evaluations of carbon fiber reinforced PEEK were done in conjunction with those of epoxy composites for comparison purposes. Typical tensile properties of a 52 percent fiber (by volume), 16 ply (2mm thick) APC-1 composite is shown in Table 4.

Processing has a strong influence on the composite properties. If the quality of the laminate is poor, low tensile properties and fatigue strength, comparable to those of epoxy composites were observed (49). A heat flow model has

Table 4. Typical Tensile Properties of APC*. 2 mm Thick, 16 Ply, 52 Percent Fiber Volume.

Composite lay-up	Tensile strength MN/m ²	Tensile modulus GN/m ²	Ultimate strain %
Uniaxial, longitudinal	1831 ± 110	122 ± 8	1.41 ± 0.04
Uniaxial, transverse ± 45°	>62 343 ± 18	9.2 ± 0.9 14.2 ± 0.4	>0.71 21 ± 2

* From Ref. 45.

been developed by Blundell and Willmough to predict the temperature profile in an APC-2 specimen which is being cooled from the melt in a molding tool held at a fixed temperature (31).

PEEK reinforced with Thornel 300 (a product of Union Carbide) was studied by Lee and Porter (25). The interfacial bond strength was measured by tensile test in the transverse direction. They found little dependency of transverse tensile strength (TTS) on the fiber content (between 11 to 32 percent fiber volume). Instead, the thermal history in the melt state seems to have a strong influence on TTS. Long holding time (100 min) at 390°C resulted in about twice as high TTS as those with short holding time (30 min). They concluded that longer melt annealing time allows stronger interfacial bondings to take place. On the other hand, transverse tensile modulus did not show dependency on the melt holding time. The transverse tensile modulus values reported by Lee and Porter are considerably lower than those reported by Jones, *et al.* (42), Cogswell and Leach (45), and Donalson (46).

Instrumented falling weight tests of quasi-isotropic layups APC (2mm thick) by Jones, *et al.* (42) revealed that the overall area of impact damage is restricted to the immediate vicinity of the impacted area, since long crack propagation is restricted by the quasi-isotropic layup. Similar tests were done by Davies, *et al.* (47) using two levels of impact energy. At a low impact energy of about 9J, no drop in impact strength of PEEK composites was observed, but that of the epoxy composite was reduced by as much as 30 percent. At the high impact energy of about 80J, catastrophic failure was observed. The type of ply sequence and method of cooling do not seem to affect the total impact energy of PEEK composites (47).

The higher impact strength of APC-2 was due to the fact that cracks initiate and propagate with more difficulty in APC-2 than in APC-1 and epoxy composites. This improvement in impact strength was again attributed to the better fiber/matrix adhesion of APC-2. The impact strengths (the peak forces of the force vs. time curves) of APC-2 and APC-1 were quoted as 6.7 ± 0.4kN and 4.5 ± 0.2kN, respectively (47). This peak force is the indication that large scale crack propagation has started to take place. The total impact energies, or the energies required

to initially punch a hole in the specimen, were reported to be $40.0 \pm 3.0\text{J}$ and $30.0 \pm 2.0\text{J}$ for APC-2 and APC-1, respectively. For comparison, the peak force and total impact energy of a presently used epoxy composite were $4.4 \pm 0.6\text{kN}$ and $25.0 \pm 2.0\text{J}$, respectively. Carlile and Leach (48) also observed the punch-through failure in APC-1, with the total impact energy proportional to thickness to the 1.42 power.

Open-hole tension testing was used to determine the notch-sensitivity (reduction in tensile strength which was caused by a through-the-thickness crack) of a specimen (48). The notch-sensitivity of APC-1 was found to be similar to that of carbon fiber reinforced epoxy composites. Compression-after-impact testing gives an indication of the damage-tolerance of a specimen. The ultimate compressive strain of undamaged APC-1 is comparable to that of undamaged epoxy composites. The residual ultimate strain of APC-1 was found to decrease gradually with increasing impact energy, with a retention of 54 percent of the undamaged strain after exposure to an impact energy of about 51J. In contrast, the residual ultimate strain of the carbon fiber-reinforced epoxy decreased sharply between 5.6 and 11.1J impact energies, with only 42 percent of the undamaged ultimate strain being retained after exposure to an impact energy of 17.5J (48).

Interlaminar fracture toughnesses (ILFT) of APC samples were measured by double cantilever beam tests (39, 45, 48). Scanning electron microscopic examination of the fracture surfaces of specimens after testing indicated that the Mode I failure of the composites consists of a slow crack growth step, where ductile deformation of the matrix took place, and a subsequent rapid crack propagation step, where only small deformation of the matrix was seen (45, 48). Similar failure mechanism was also reported by Hartness (39). There are discrepancies in the reported values of the G_{IC} of the steps, however. Hartness reported the G_{IC} values of about 1.75kJ.m^{-2} and 1.4kJ.m^{-2} for the slow crack growth and the crack propagation steps, whereas Leach, *et al.* (45, 48) found the respective values to be 3.2kJ.m^{-2} and 1.87kJ.m^{-2} . For comparison, the average ILFT of a typical epoxy composite is about 210J.m^{-2} . The excellent ILFT of APC is the result of the combination of a ductile PEEK matrix and a good fiber/matrix interfacial adhesion.

The Mode II (forward shearing) and mixed mode (off-axis tensile) failures of APC-1 composite specimens were investigated by Donalson (46). In Mode II, crack growth starts suddenly and propagates in an unstable manner. In the mixed mode failure, ductile spike formations in the direction of the applied shear were observed in fractographs which may account for the good ILFT of the PEEK composites.

Since they offer the possibility of having no weak transverse direction and higher fracture

toughness with thinner laminates, directly impregnated woven carbon fabrics have been made following the same procedure as the one used to produce APC. The quality of PEEK laminates was improved as consolidation pressure was increased (50). Fatigue tests in the tension-tension mode indicated that PEEK reinforced with Thorne 300 carbon cloth (54 percent fiber volume) was less sensitive to fatigue than epoxy reinforced with the same cloth (50) (the slope of the S-N curve of PEEK was smaller compared to that of the state-of-the-art epoxy). This superior fatigue resistance was attributed mainly to the resistance of PEEK to the initiation and propagation of fatigue cracks (51). However, the tensile strength of PEEK reinforced with carbon cloth could be lower than those of comparable cross ply (0/90) laminates (52).

EFFECTS OF ENVIRONMENTS

Since PEEK and its composites are being actively evaluated for high performance applications, it is essential that their performances in hostile environments are understood. There have been investigations on the effects of physical and thermal agings, moisture, solvents, and radiation on the structure, physical, and mechanical properties of PEEK and its composites.

Physical and Thermal Agings

Physical aging of amorphous and semicrystalline polymers is the gradual change of properties of the polymers with time at temperature below their glass transitions. In general, when an amorphous polymer undergoes physical aging, its free volume decreases, its tensile yield stress and degree of brittleness increase, and its creep behavior changes.

Physical aging (annealing below T_g) of amorphous PEEK ($T_g = 145^\circ\text{C}$) revealed that there is a relaxation mechanism which occurs in the temperature range 50 to 140°C (30). This secondary viscoelastic molecular motion, which involves the partial bond rotation of the ether linkages, aligns the diphenyl ether groups into ordered regions. Then above T_g , a second mechanism, which is associated with crystallization and requires the motion of the whole polymer chains, takes place. Its onset is signified by the rotation of the ketone linkages at about 140°C . Kemmish and Hay (18) found physical aging to have no effect on the heat capacities of PEEK except in the T_g region, where an endothermic peak was observed (Fig. 14). The magnitude of this endothermic process increased logarithmically with time. The molecular weight of PEEK was found to change the rate of physical aging only by changing T_g .

Mechanical properties of neat PEEK were found to be greatly affected by physical aging (18). Tensile yield stress increased from 59MPa (amorphous polymer) to as high as 75MPa. Elastic modulus increased slightly while impact

strength decreased from 85 kJ.m^{-2} to 7.3 kJ.m^{-2} . Necks were seen to form upon deformation, but their appearances were different from those due to crystallization. The fractured surfaces of notched specimens showed little deformation with a craze zone close to the notch. A ductile-brittle transition was also observed with progressive aging.

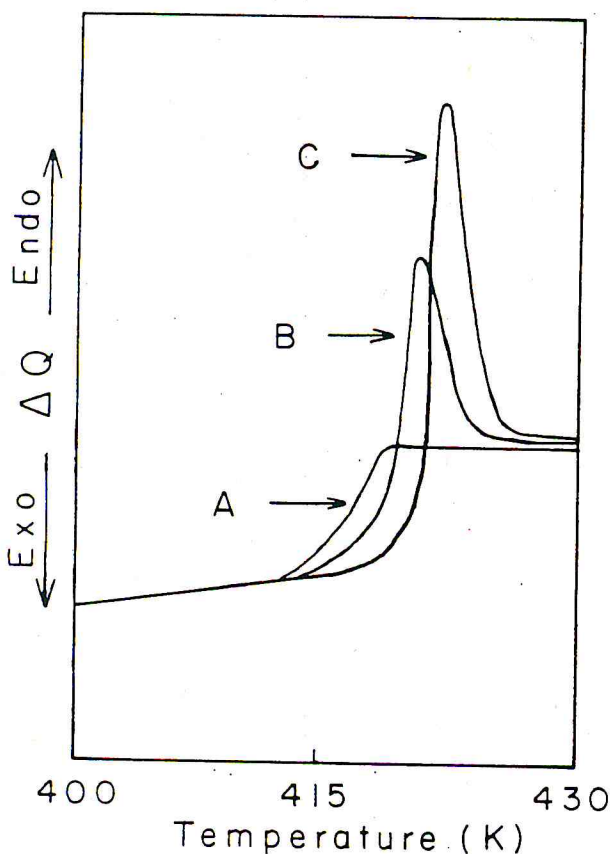


Fig. 14. DSC thermograms showing the effect of aging in the T_g region: (A) quenched sample; (B) aged for 4 h; (C) aged for 32 h. Samples were annealed at 10°C below T_g . From data of Kemmish and Hay (18).

The effects of physical aging (below T_g) and thermal aging (above T_g) on APC-1 have been studied (39, 45). As expected, the effects were found to be greater on matrix-dominated properties such as transverse and $\pm 45^\circ$ tensile properties. Tensile tests of the composites were done at 121 and 177°C by Hartness (39). Moderate drops were observed in tensile strength, modulus, and ultimate elongation in the longitudinal direction. In the transverse direction, the drop in tensile strength and modulus were severe, but ultimate strain increased by 253 percent at 121°C and 578 percent at 177°C , indicating that the PEEK matrix became more rubbery at elevated temperatures. The changes in $\pm 45^\circ$ tensile properties are intermediate. Cogswell and Leach (45) also measured tensile properties at 80 and 120°C for $\pm 45^\circ$ lay-up specimens. The values they reported are listed with those obtained by Hartness in Table 5.

Cogswell and Hopprich (54) conditioned specimens of APC-1 in vacuo for one day at 100°C . These samples retained about 81 percent of the short beam shear strength of the unaged ones. When the samples were tested in flexure at 100°C , their flexural strength dropped by 1 percent while their flexural modulus increased by about 6 percent. Flexural strength and modulus of APC-1 were also measured at different temperatures ($22, 121, 149$, and 177°C) by Hartness (39). Both unaged and aged ($150^\circ\text{C}, 1000$ h) samples were evaluated. The results, which agreed well with those measured by Cogswell and Hopprich, are presented in Table 6. Considerable plastic deformation of the matrix was observed at elevated temperatures. In most cases, severe drops in flexural properties did not occur until the test temperatures were well above T_g . Cogswell and Leach (45) studied the effects of exposure time of physical aging (120°C) and thermal aging (220°C) on the transverse flexural strength of APC-1. For samples

Table 5. Retention of Tensile Properties of APC at Elevated Temperatures*.

	Retention of tensile strength (%)			Retention of tensile modulus (%)			Retention of ultimate strain (%)	
	80°C	121°C	177°C	80°C	121°C	177°C	121°C	177°C
Longitudinal	82	78			91	92	.88	82
Transverse	55	39			53	16	253	578
$\pm 45^\circ$	84 ^a	76/57 ^b	63	92 ^a	71/78 ^b	21	92	107

* Ref. 45.

^b Ref. 45, test was done at 120°C .

^a Calculated from Ref. 39.

Table 6. Retention of Flexural Properties of APC at Elevated Temperatures*.

	Retention of flexural strength (%)				Retention of flexural modulus (%)			
	22°C	121°C	149°C	177°C	22°C	121°C	149°C	177°C
Longitudinal	100	79	56	41	100	105	86	72
Transverse	100	94	65	50	100	114	78	46
Thermally aged longitudinal	103	76	68	45	107	104	103	84
Thermally aged transverse	88	79	59	—	86	52	—	—

* Calculated from Ref. 39.

conditioned at 120°C, flexural strength dropped slightly (to 90 to 98 percent of that of unaged samples) after 4 min of exposure, but then no further reduction was seen. However, samples aged at 220°C gradually lost their transverse flexural strength, with a retention of only 70 percent after 1320 h. Changes in the mechanical properties, especially flexural properties, of APC-1 due to physical aging reflect the structural changes of neat PEEK due to relaxation below T_g .

Effect of Moisture

Very little effect of moisture on the properties of injection molding grades of PEEK was seen (54, 55). Less than 0.1 percent weight gain was detected when neat polymer films were either immersed in deionized water at 20 and 70°C (55) or conditioned in air at about 70 percent RH for 7 days (56). After 30 days in water at 80°C, tensile strength of the neat polymer was found to increase by 5 percent. A decrease of 5 percent in tensile strength was observed after 322 days in 100°C water. After 30 min in 288°C water, which was pressurized at 180 MPa, neither obvious signs of degradation nor change in dimensions of the samples was detected.

The absorption of moisture by carbon fiber reinforced PEEK composites was found to depend on the grade of PEEK and the conditions at which moisture aging was carried out. Hartness (39) immersed specimens of APC-1 in water at 70°C and found that the equilibrium moisture uptake was only 0.2 percent by weight. Other work on APC-1 reported 0.25 and 0.45 percent weight gain in boiling water after about 3 days (54) and 3 weeks (49), respectively.

Comparison of dynamic mechanical spectra (Fig. 15) of moisture-aged and dry specimens of neat PEEK revealed a difference in the very broad, low temperature γ transition (from -130 to 30°C) (56). For moisture aged samples, three peaks were observed in this region, -100, -80, and -40°C. Upon drying, the peak at -100°C disappeared while the ones at -80 and -40°C remained. This -100°C peak is thought to be associated with rotational movements of absorbed water molecules which form complexes with the phenyl ketone moieties (56).

APC-1 samples aged in air at 65 percent RH showed a weight gain of only 0.08 percent after 1000 h (49). On the other hand, specimens of a CFR composite of a film-grade PEEK (containing 57 percent by volume of fiber) showed a water absorption of 0.4 percent by weight after moisture aging to equilibrium at 70°C (53). Shot-blasting the surface of APC-1 laminate did not seem to affect moisture absorption (49).

As in the case with thermal aging, moisture was found to have little effect on longitudinal properties, but have strong influence on the transverse properties. The tensile fatigue resistance of cross-ply APC-1 laminates was

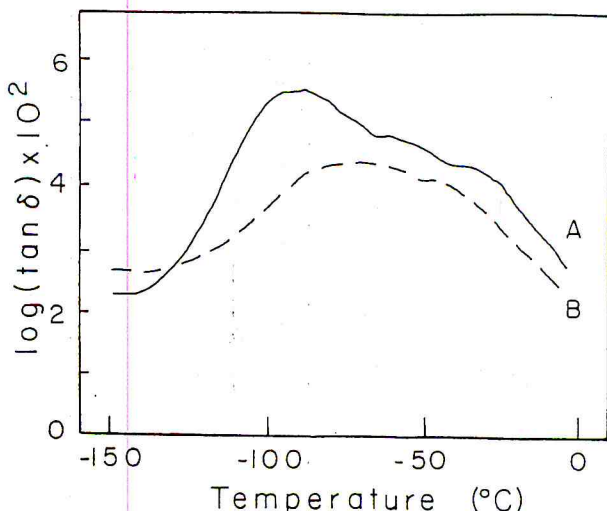


Fig. 15. Effect of moisture as seen in the γ transition region of dynamic mechanical spectra of amorphous PEEK samples: (A) moisture-aged; (B) dry. Reproduced from (56).

found to be unaffected by moisture level or by hydrothermal aging (boiling water immersion) treatment (49). Flexural strength and modulus in the longitudinal direction slightly improved after the composite specimen has been moisture-aged to equilibrium in 70°C water. However, transverse flexural properties (strength, modulus, and strain at break) decreased by more than 10 percent (39). The combined effect of moisture aging and testing at elevated temperatures on flexural properties of APC-1 was found to be severe if the testing was done at 120°C or higher. When tested at 100°C, samples aged for 24 h in 95°C water showed slight improvements in flexural strength and modulus (54). When tests of samples moisture-aged at 70°C were carried out at 120 and 180°C, only 84 and 59 percent of the flexural strength at room temperature were retained, respectively (53). Similar drops in longitudinal and transverse flexural properties when testings were done at 121, 149, and 177°C have also been shown (39). Since it has been observed that the flexural strengths of wet and dry samples were almost identical at temperature above 100°C (53, 54), moisture absorption of carbon fiber reinforced PEEK composites may be a reversible process.

Effects of Solvents

Stober, *et al.* studied the effects of an aviation hydraulic test fluid (Skydrol) at 20 and 70°C, and of methylene chloride at 20 and 36°C on PEEK films (55). Specimens having two different crystalline contents (7.6 and 25.8 percent) were used.

The absorption of Skydrol was found to be moderate, with the higher temperature causing faster absorption and higher equilibrium weight gains. Weight gains of 0.6 percent at 20°C and 1.7 percent at 70°C were found for the less crystalline specimens, whereas gains of 0.8 and

1.1 percent were reported for the more crystalline specimens. These amounts of absorbed Skydrol did not affect the dimensional stability (by thermomechanical analysis) or crystalline content (by density column measurement) of individual specimens. The absorption of Skydrol was reversible. It was found that essentially complete desorption could take place at room temperature in a vacuum of 0.11 Torr. Thus, PEEK can be considered as highly resistant to Skydrol.

The effect of methylene chloride is not yet clear. Large quantities of the solvent were absorbed by PEEK. At the higher temperature, faster absorption but lower equilibrium weight gains were observed. At 20°C, weight gains of 20.8 and 15.4 percent were found for specimens with lower and higher degrees of crystallinity, respectively. The corresponding weight gains were 19.7 and 15.2 percent at 36°C. Absorptions by single ply APC-1 specimens were found to be very similar to that of the more crystalline specimens of neat PEEK. The absorption of methylene chloride may be irreversible: complete desorption could not be achieved, about 1 percent by weight of residual solvent was found in each specimen. The absorbed solvent was shown to have plasticizing effects below T_g , and to induce crystallization in PEEK. This phenomenon may be described as solvent aging. Below T_g , samples with absorbed methylene chloride showed lower elastic moduli. Upon desorption, moduli and T_g higher than those of the original samples were observed (55). The magnitude of the T_g peak in the dynamic mechanical spectrum was reduced by the presence of methylene.

Cogswell and Hopprich (54) evaluated the performance of APC-1 in the presence of various solvents. After 7 days at 23°C in common solvents such as acetone, methyl ethyl ketone, cyclohexane, kerosene, and gasoline, no change in weight was observed with about 95 percent retention of the original tensile strength and modulus. In aircraft hydraulic fluids and synthetic lubricants, 95 percent of the flexural modulus and 90 percent of the flexural strength were retained after exposure of 1 month at 23°C. Exposure to a paint stripper (1 month, 23°C) resulted in slight increases in flexural strength (6 percent) and flexural modulus (1 percent), and no change in short beam shear strength. About 1 percent weight gain and about 5 percent reduction in tensile strength and ultimate elongation were detected after 1 week in concentrated ammonium hydroxide at 23°C.

Environmental stress cracking tests were also carried out at 0.9 percent and 23°C in acetone, trichloroethylene, ethyl acetate, isopropyl alcohol, n-hexane, and jet fuels (54). Cracks were not observed after 20 min of exposure.

Inspections of dynamic mechanical spectra of

neat PEEK indicated that absorbed solvents such as methylene chloride cause some conformational changes. For semi-crystalline specimens, a low-magnitude peak (β' transition) was observed at around 85°C. Upon absorption of methylene chloride, this transition was depressed. It reappeared after methylene chloride was desorbed (Fig. 16) (55). It is interesting to compare the effect of solvent on this transition with the molecular relaxation process due to physical aging observed by Nguyen and Ishida (30). It seems that the effects of physical aging and mild solvent attacks are similar at the molecular level.

Effect of Radiation

At the present, only the effect of electron beam irradiation has been well characterized. PEEK from Sumitomo Kagaku Kogyo Co., Ltd. was used in these studies. Techniques to quantify the radiation damage included dynamic mechanical analysis, X-ray diffraction, DSC, and tensile testings.

Sasuga and Hagiwara (56) used dynamic viscoelastic properties in the torsion mode as indicators of damages due to radiation dosages of 1000, 3000, and 5000 Mrad. A number of changes at the molecular level were inferred from the dynamic mechanical spectra (Fig. 17).

In the γ transition region (-120 to 30°C), the shoulder at -40°C disappeared after irradiation but then reappeared upon melting, cooling, and reheating. This was interpreted as the destruction of an inherent chain conformation which gives rise to local order in the amorphous regions by electron radiation.

The β' transition (between 40 and 120°C) appeared after irradiation, but was then depressed by subsequent melting, cooling, and reheating. Its magnitude increased with increasing radiation dosage. This transition was also observed

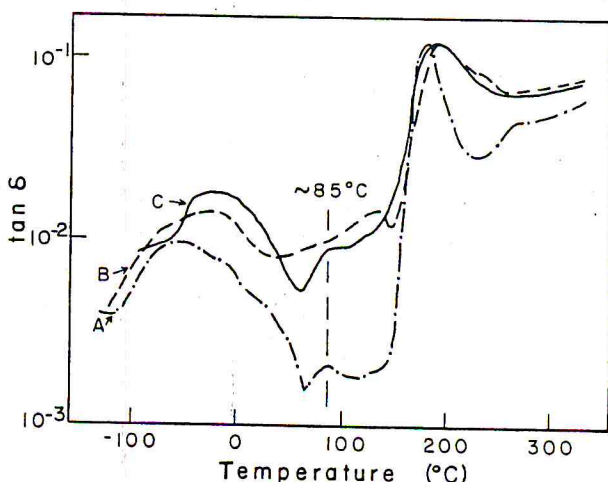


Fig. 16. Conformational changes due to the absorption of methylene chloride observed in dynamic mechanical spectra of semi-crystalline PEEK: (A) before absorption of solvent; (B) after absorption; (C) after desorption of solvent. Reproduced from data of Stober, et al. (55).

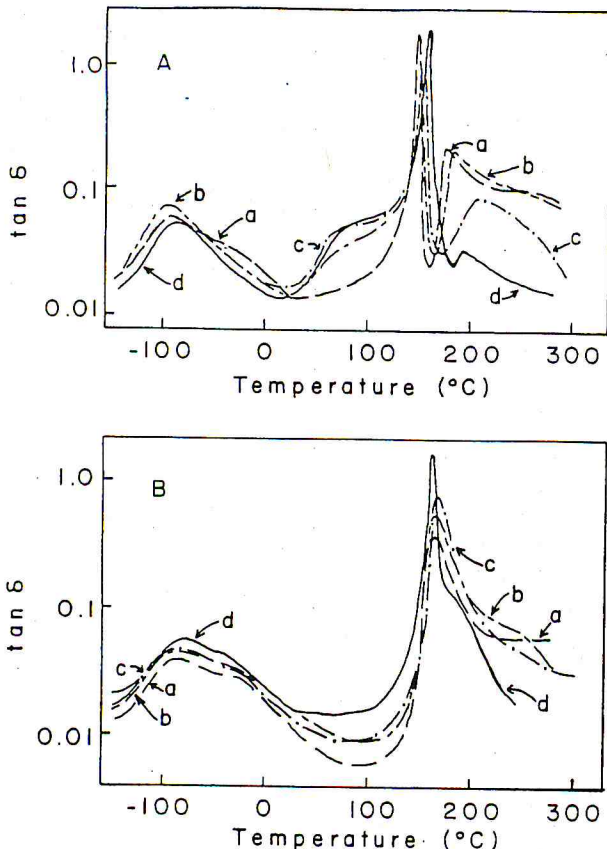


Fig. 17. Effect of electron beam radiation on the loss tangent of semi-crystalline PEEK samples: (a) no radiation; (b) 1000 Mrad; (c) 3000 Mrad; (d) 5000 Mrad. (A) after radiation exposure; (B) after subsequent melting and cooling. Reproduced from data of Sasuga and Hagiwara (56).

in dynamic mechanical spectra of amorphous PEEK, which disappeared as the polymer became more crystalline. It was associated with the partial rotation of the ether linkages in the amorphous domains to achieve better chain packing (30). Hence, it was concluded that radiation causes chain scission and allows the newly created chain ends to loosen molecular packing to the level of amorphous polymer. X-ray diffraction data by Yoda (58) supported this conclusion. He found that even though the unit cell and lattice distortion seemed to be unaffected by irradiation, crystal size decreased almost linearly with increasing radiation dosage (Table 7). Since the long period was found to be unchanged, the amorphous region must have been thickened by the new chain ends.

The glass transition β (around 145°) was shifted slightly to higher temperatures with irradiation. Its magnitude increased with increasing radiation dosage. This may indicate that formation of crosslinks (instead of induced crystallization as in the case of solvent attack).

Crystallization via annealing was reduced significantly by radiation exposure. $T_{c,h}$ could no longer be observed by DSC after 5000 Mrad exposure (57). In addition, this α' transition ($\sim 180^\circ\text{C}$) was shifted to higher temperatures

Table 7. Effect of Electron Beam Radiation on Crystal Size, Crystallization Temperature ($T_{c,h}$), and Melting Temperature (T_m).

Dose (Mrad)	Crystal size (nm)	$T_{c,h}$ (°C)	T_m (°C)
0	6.1	175	335
1000	5.8	185	320
3000	5.7	205	305
5000	5.3	not observed	not observed

(Table 7). Annealing of specimens which have been exposed to 3000 Mrad could achieve a maximum crystalline content of 30 percent (57). Crosslinking could explain this behavior of the crystallization peak.

T_m , as observed in the shear modulus vs. time curves, was lowered by irradiation. DSC data indicated that this α transition dropped from 335°C (no radiation) to 320°C (1000 Mrad) and 305°C (3000 Mrad), until it could not be detected after 5000 Mrad exposure (Table 7) (57). X-ray diffraction data confirmed that specimens which were previously subjected to 5000 Mrad dosage became completely amorphous (57). Attempts to anneal them at up to 300°C failed to induce any crystallinity.

Thus, degradation by high energy electron beam radiation may induce chain scission and crosslinking simultaneously. This combined effect loosens PEEK's crystal structure and reduces its ability to crystallize. Electron beam degradation may occur only near the surface of PEEK lamellae.

Tensile properties of amorphous and 15 percent crystalline PEEK specimens as functions of irradiation dosages were measured by Sasuga, *et al.* (59). They found that amorphous samples were affected more significantly than crystalline ones, with the exception of ultimate elongation. The results of Sasuga, *et al.* are reproduced in Fig. 18 (yield and ultimate tensile strengths vs. dosage) and Fig. 19 (ultimate elongations vs. dosage). After an amorphous sample was exposed to 5000 Mrad, its elastic modulus increased by 21 percent, while its yield tensile strength, ultimate tensile strength, and ultimate elongation decreased by 21, 57, and 82 percent, respectively. For a semi-crystalline sample exposed to the same dosage, the elastic modulus increased by only 1 percent, while the reductions in yield strength, ultimate strength, and ultimate elongation were 7, 13, and 85 percent, respectively.

OTHER DEVELOPMENTS

From the works on molecular weight determination of PEEK (12, 13), it was apparent that PEEK became sulfonated upon dissolution in concentrated sulfuric acid. Sulfonation was found to occur exclusively in the oxy-1,4-phenylene-oxy rings (phenyl rings which are surrounded by 2 ether linkages) (12, 60) to an equilibrium degree of one $-\text{SO}_3\text{H}$ per structural

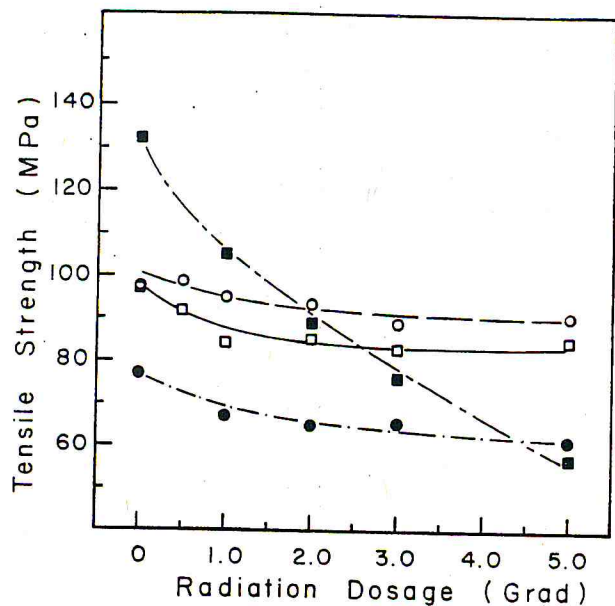


Fig. 18. Effect of radiation on the tensile strengths of PEEK: (○) yield strength of semi-crystalline samples; (●) yield strength of amorphous samples; (□) ultimate strength of semi-crystalline samples; (■) ultimate strength of amorphous samples. From data of Sasuga, et al. (59).

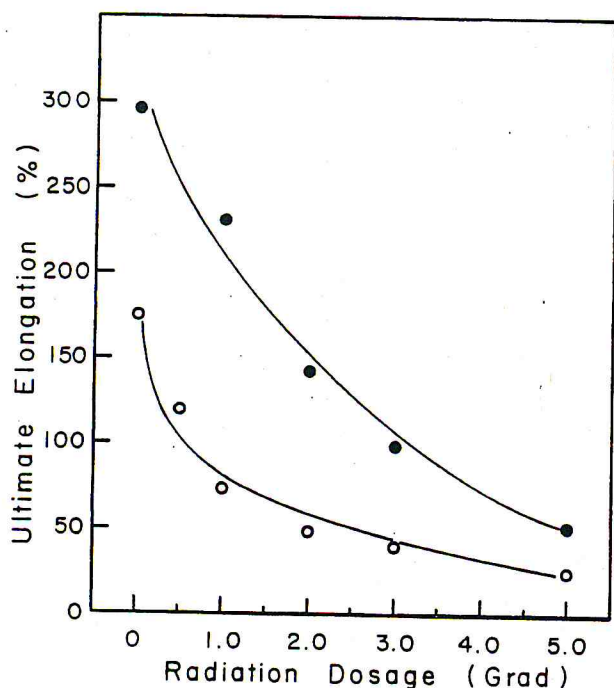


Fig. 19. Effect of radiation on elongation at break: (○) semi-crystalline (●) amorphous. From data of Sasuga, et al. (59).

repeat unit. Some crosslinking may occur in 100 percent H_2SO_4 (13). Sulfonation alters the chain packing, thus drastically reduces the crystalline content and the crystallization rate of PEEK. However, T_g is increased. At a sulfonation level of 0.72 (the concentration of $-SO_3H$ is 0.72 group per repeat unit of PEEK), a fully amorphous polymer with $T_g = 206^\circ C$ was ob-

tained (60). Sulfonation was also found to decrease the thermal stability of PEEK significantly. Neutralization of the sulfonated PEEK with metal such as Na or Zn improved thermal stability, but the neutralized material was still not as thermally stable as PEEK. Poorer melt processability was also observed.

Crosslinking of PEEK with elemental sulfur has been carried out (61). When sulfur was compounded with PEEK, polymer chain scission was found to occur first. Upon aging at temperatures above T_g , crosslinking took place. The degree of crosslinking was found to increase with higher annealing temperature. Higher T_g improved creep resistance, and better tensile properties at temperatures above T_g were found to be the results of this crosslinking technique (61).

Another approach to improve the performance of PEEK has been proposed by Wu, et al. (62). In an attempt to combine the most desirable properties of PEEK and aromatic polysulfones, they synthesized a number of random and segmented poly(aryl-ether-ketone-sulfone) copolymers. In general, the resultant polymers were found to be either a) amorphous with T_g from 20 to 60°C higher than that of PEEK or b) semi-crystalline with higher T_g but lower T_m than those of PEEK. However, a segmented polymer made from the polymerization of bisphenol-based polysulfone oligomers with bisphenol and 4,4'-difluorobenzophenone (21:35:44 in weight proportions) was found to be semi-crystalline with $T_g = 181^\circ C$ and $T_m = 387^\circ C$. These copolymer were found to be solvent resistant and ductile, as expected.

CONCLUDING REMARKS

We have summarized the published studies of PEEK and its composites. Interestingly, it was found that aside from its high melting point, lack of solubility in common solvents, and exceptional mechanical properties, PEEK is very similar to other semi-crystalline polymers in many aspects such as solution behavior, morphology, environmental resistances, and fracture behavior. However, PEEK does have a number of distinctive characteristics. Previous thermal history is very influential to the melting and crystallization behavior of the polymer. PEEK forms folded chain lamellae upon crystallization, but because of the rigidity of the chains and the distance between the ether and ketone linkages, the noncrystalline layers are thick. The result is the inherently low degree of crystallinity of PEEK. The polymer tends to assume orientation upon crystallization on crystalline substrates. The orientation of the chains and the crystal lamellae seems to depend upon the thickness of the polymer layer. But how orientation changes with thickness is still unclear.

ACKNOWLEDGMENT

This work was supported in part by the Office of Naval Research.

REFERENCES

1. T. C. Stening, C. P. Smith, and P. J. Kimber, *Mod. Plast.*, 86 (Nov. 1981).
2. D. J. Willats, *SAMPE J.*, 20, 6 (1984).
3. V. Wigotsky, *Plast. Eng.*, 42, 17 (1986).
4. R. N. Johnson, A. G. Farnham, R. A. Clendinning, W. F. Hale, and C. N. Merriam, *J. Polymer Sci.*, A-1, 5, 2375 (1967).
5. J. B. Rose, *Am. Chem. Soc., Div. Polym. Chem., Polym. Prepr.*, 27, 40 (1986).
6. T. E. Attwood, P. C. Dawson, J. L. Freeman, L. R. J. Hoy, J. B. Rose, and P. A. Staniland, *Polymer*, 22, 1096 (1981).
7. H. R. Kricheldorf, and G. Bier, *Polymer*, 25, 1151 (1984).
8. J. B. Rose, and P. A. Staniland, *US Pat.* 4 320 224 (1982).
9. H. X. Nguyen, and H. Ishida, *Die Makromol. Chem./Macromol. Symp.*, Vol. 5, 135 (1986).
10. A. J. Lovinger, and D. D. Davis, *Polymer (Commun.)*, 26, 322 (1985).
11. J. Del Rios, *J. Analysis Purification*, 21 (March, 1986).
12. J. Devaux, D. Delimoy, R. Legras, J. P. Mercier, C. Strazielle, and E. Nield, *Polymer*, 26, 1994 (1985).
13. M. T. Bishop, F. E. Karasz, P. S. Russo, and K. H. Langley, *Macromolecules*, 18, 86 (1985).
14. D. J. Blundell, and B. N. Osborn, *Polymer*, 24, 953 (1983).
15. H. X. Nguyen, and H. Ishida, *Am. Chem. Soc., Div. Polym. Chem., Polym. Prepr.*, 26, 273 (1985).
16. H. X. Nguyen, and H. Ishida, *Polymer*, 27, 1400 (1986).
17. H. X. Nguyen, *Ph.D. Dissertation*, Case Western Reserve University, Cleveland, Ohio (1986).
18. D. J. Kemmish, and J. N. Hay, *Polymer*, 26, 905 (1985).
19. P. Cebe, *Am. Chem. Soc., Div. Polym. Chem., Polym. Prepr.*, 27, 449 (1986).
20. H. X. Nguyen, and H. Ishida, unpublished data.
21. R. B. Whitaker, A. B. Nease, and R. O. Yelton, *U.S. D.O.E. Report MLM-3141* (1984).
22. J. N. Hay, D. J. Kemmish, J. I. Langford, and A. I. M. Rae, *Polymer (Commun.)*, 25, 175 (1984).
23. S. Kumar, D. P. Anderson, and W. W. Adams, *Polymer*, 27, 329 (1985).
24. D. J. Blundell, J. M. Chalmers, M. W. Mackenzie, and W. F. Gaskin, *SAMPE Quarterly*, 16, 22 (1985).
25. Y. C. Lee, and R. S. Porter, *Office of Naval Research. Tech. Report No. 26* (1985).
26. J. M. Chalmers, W. F. Gaskin, and M. W. Mackenzie, *Polymer Bull.*, 11, 433 (1984).
27. J. D. Louden, *Polymer (Commun.)*, 27, 82 (1986).
28. J. N. Clark, F. G. Herring, and N. R. Jagannathan, *Polymer (Commun.)*, 26, 329 (1985).
29. F. N. Cogswell, *28th Natl. SAMPE Symp.*, 28, 528 (1983).
30. H. X. Nguyen, and H. Ishida, *J. Polym. Sci., Polym. Phys. Ed.*, 24, 1079 (1986).
31. D. J. Blundell, and F. Willmouth, *SAMPE Quarterly*, 17, 50 (1986).
32. A. J. Lovinger, and D. D. Davis, *J. Appl. Phys.*, 58, 2843 (1985).
33. R. H. Olley, D. C. Bassett, and D. J. Blundell, *Polymer*, 27, 344 (1986).
34. P. C. Dawson, and D. J. Blundell, *Polymer*, 21, 577 (1980).
35. D. R. Rueda, F. Ania, A. Richardson, I. M. Ward, and F. J. Balta Calleja, *Polymer (Commun.)*, 24, 258 (1983).
36. N. T. Wakelyn, *Polymer (Commun.)*, 25, 306 (1984).
37. D. A. Luippold, *30th Natl. SAMPE Symp.*, 30, 809 (1985).
38. A. Lustiger, *SAMPE J.*, 20, 13 (1984).
39. J. T. Hartness, *SAMPE J.*, 20, 26 (1984).
40. A. J. Lovinger, and D. D. Davis, *Bull. Am. Phys. Soc.*, 30, 249 (1985).
41. P. S. Pao, J. E. O'Neal, and C. J. Wolf, *Polym. Mater. Sci. Eng. Proc.*, 53, 677 (1985).
42. D. P. Jones, D. C. Leach, and D. R. Moore, *Polymer*, 26, 1385 (1985).
43. S. S. Yau, and T. W. Chou, *30th Natl. SAMPE Symp.*, 30, 406 (1985).
44. J. F. Mandel, F. J. McGarry, D. D. Huang, and C. G. Li, *Polym. Compos.*, 4, 38 (1983).
45. F. N. Cogswell, and D. C. Leach, *Plast. Rub. Proc. Appl.*, 4, 271 (1984).
46. S. L. Donaldson, *Composites*, 16, 103 (1985).
47. C. K. L. Davies, S. Turner, and K. H. Williamson, *Composites*, 16, 279 (1985).
48. D. R. Carlile, and D. C. Leach, *15th Natl. SAMPE Tech. Conf.*, 15, 82 (1983).
49. R. F. Dickson, C. J. Jones, B. Harris, D. C. Leach, and D. R. Moore, *J. Mater. Sci.*, 20, 60 (1985).
50. T. Y. Hartness, and R. Y. Kim, *28th Natl. SAMPE Symp.*, 28, 535 (1983).
51. R. Y. Kim, and J. T. Hartness, *29th Natl. SAMPE Symp.*, 29, 765 (1984).
52. U. Measuria, and F. N. Cogswell, *SAMPE J.*, 21, 26 (1985).
53. J. T. Hartness, *14th Natl. SAMPE Tech. Conf.*, 14, 26 (1982).
54. F. N. Cogswell, and M. Hopprich, *Composites*, 14, 251 (1983).
55. E. J. Stober, J. C. Seferis, and J. D. Keenan, *Polymer*, 25, 1845 (1984).
56. T. Sasuga, and M. Hagiwara, *Polymer*, 26, 501 (1985).
57. O. Yoda, *Polymer (Comm.)*, 25, 238 (1984).
58. O. Yoda, *Polymer (Comm.)*, 26, 16 (1985).
59. T. Sasuga, N. Hayakawa, K. Yoshida, and M. Hagiwara, *Polymer*, 26, 1039 (1985).
60. X. Jin, M. T. Bishop, T. S. Ellis, and F. E. Karasz, *British Polym. J.*, 17, 4 (1985).
61. S. Venkatraman, and C. M. Chan, *Am. Chem. Soc., Div. Polym. Chem., Polym. Prepr.*, 27, 305 (1986).
62. S. D. Wu, J. L. Hedrick, B. K. Carter, D. K. Mohanty, E. Yilgor, G. L. Wilkes, and J. E. McGrath, *Am. Chem. Soc., Div. Polym. Chem., Polym. Prepr.*, 26, 277 (1985).